Controlled Synchronization of Heterogeneous Robotic Manipulators in the Task Space

Yen-Chen Liu and Nikhil Chopra

***Abstract*—Passivity-based control has emerged as an important paradigm for synchronization of networked robotic systems. Despite the practical utility of task space algorithms, the previous results focussed on joint space synchronization, and were primarily derived for kinematically identical manipulators. Hence, in this paper the problem of task space synchronization of (possibly redundant) heterogeneous robotic systems is studied. By exploiting passivity based synchronization results developed previously, an adaptive control algorithm is proposed to guarantee task space synchronization of networked robotic manipulators in the presence of dynamic uncertainties and time-varying communication delays. To demonstrate the efficacy of proposed framework, numerical simulations and experiments are conducted with redundant and non-redundant manipulators respectively.**

***Index Terms*—Synchronization, Time-varying Delay, Task Space Tracking, Redundant Manipulator**

I. Introduction

The design of control algorithm, and/or artificial interconnections to synchronize a group of interconnected dynamical systems is known as controlled synchronization [1]. Controlled synchronization between multiple manipulators can lead to high performance control algorithms, for example, in production processes where high flexibility, manipulability, and maneuverability are desirable characteristics. Controlled synchronization for robotic systems was first proposed in [2], where the manipulators were controlled to follow a desired trajectory, and mutual synchronization between the robotic systems was utilized to enhance the performance of the closed loop system. As the proposed algorithm required all-to-all coupling between the agents, the control scheme did not scale well with the number of robots. Subsequently, contraction theory was utilized [3] to guarantee synchronization and tracking on regular graphs. The authors also applied their theoretical results for synchronization of formation flying spacecraft in [4]. A passivity-based algorithm for synchronization and tracking of mechanical systems on balanced communication graphs was studied in [5]. The various advantages of controlled synchronization have been well discussed in the aforementioned papers [2]–[5].

The passivity and the dissipativity paradigm were used to study the synchronization problem in [6]–[8]. Specifically, it was demonstrated in [8], [9] that nonlinear passive systems can be output synchronized, provided the storage function is positive definite, and the interagent communication graph is balanced. These results were successfully applied to joint space synchronization of bilateral teleoperators [10]. Building on this work, scaled synchronization of bilateral teleoperators with different configurations was proposed in [11]; however, the authors considered motion control of kinematically identical, and non-redundant robotic systems. Motivated the possible performance benefits of redundant systems, teleoperation of redundant manipulators was studied in [12]. However, the master and slave robots were required to have the same degrees-of-freedom, and communication unreliabilities (e.g. time delays) between the robotic systems were not considered.

This work was supported by the National Science Foundation under grant 0931661.

Y.-C. Liu is with the Department of Mechanical Engineering, University of Maryland, College Park, MD 20742 USA (e-mail:yliu0925@umd.edu).

N. Chopra is with Faculty of Department of Mechanical Engineering and the Institute for Systems Research, University of Maryland, College Park, MD 20742, USA (e-mail:nchopra@umd.edu).

In this paper, we study controlled synchronization of heterogeneous robotic manipulators in the task space. By demonstrating that the task space tracking control developed in [13], [14] is input-output passive, the output synchronization results in [8] are utilized to synchronize robotic manipulators in the task space. Under the assumption that the communication graph between the agents is balanced and strongly connected, the tracking and synchronizing errors are guaranteed to converge to the origin. In contrast to [10]–[12], where joint space synchronization between two robotic systems was studied, we develop task space synchronization algorithms for multiple non-redundant and redundant manipulators. Additionally, redundancy in the manipulators is also exploited for achieving sub-tasks [15], such as increased manipulability in the workspace.

It is well known that time delays in the feedback loop, for example when the control signals are communicated over unreliable networks, can destabilize the closed loop system [16]. The problem of synchronization with time delays has been studied in [3], [5], [8], [9], where the time delays were assumed to be constant and bounded. However, in networked multi-robotic systems, the communication delays may be time-varying with possibly unknown statistics. To address this issue, the problem of task space synchronization with time-varying communication delays is also studied. Based on the assumption that the maximum rate of change of delays is less than one, a control algorithm is proposed for delay independent task space synchronization of heterogeneous robotic manipulators.

The rest of the paper is organized as follows. The relevant background is discussed in Section II, which is followed by the results of task space synchronization in Section III. The output synchronization problem in the presence of time-varying delays in the communication channel is studied in Section IV. In Section V, simulation and experimental results are presented to demonstrate the efficacy of the proposed control algorithms. Finally, the conclusions are made in Section VI, and avenues for future research are also discussed.

II. Preliminaries

Following [17], in the absence of friction, the Euler-Lagrange equations of motion for an n-degree-of-freedom robotic manipulator are given as

$$M(q)\ddot{q} + C(q,\dot{q})\dot{q} + g(q) = u, \tag{1}$$

where $q \in R^n$ is the vector of generalized configuration coordinates, $u \in R^n$ is the vector of generalized forces acting on the system, $M(q) \in R^{n\times n}$ is a symmetric, positive definite matrix, $C(q,\dot{q})\dot{q} \in R^n$ is the vector of Coriolis/Centrifugal forces, and $g(q)=\frac{\partial G}{\partial q} \in R^n$ is the gradient of the potential function $G(q)$. In this paper, the analysis is focused on manipulators with revolute joints. Therefore, the above equations exhibit certain fundamental properties due to their Lagrangian dynamic structure [17].

- **Property 1:** The matrix $M(q)$ is positive definite and there exists positive constants λ_m and λ_M such that

$$\lambda_m I \leq M(q) \leq \lambda_M I. \tag{2}$$

- **Property 2:** For any differentiable vector $\xi \in R^n$, the Lagrangian dynamics are linearly parameterizable which gives that

$$M(q)\dot{\xi} + C(q,\dot{q})\xi + g(q) = Y(q,\dot{q},\xi,\dot{\xi})\Theta, \tag{3}$$

  where $\Theta \in R^k$ is a set of dynamic parameters and $Y \in R^{n\times k}$ is a matrix of known functions of the generalized coordinates and their higher derivatives.
- **Property 3:** Under an appropriate definition of the matrix C, the matrix $\dot{M}$ - $2C$ is skew symmetric.

Let $X \in R^m$ represent the position of the end-effector in the task space. It is related to the joint space vector q as

$$X = h(q) \quad , \quad \dot{X} = J(q)\dot{q}, \tag{4}$$

where $h(\cdot) : R^n \rightarrow R^m$ denotes the mapping between the joint space and the task space, and $J(q) = \partial h(q)/\partial q \in R^{m\times n}$ is the Jacobian matrix. In this paper, the Jacobian is assumed to be known; future work will incorporate adaption schemes as proposed in [18], [19].

For the multi-agent system, the communication topology and information exchange between the agents can be represented as a graph. The reader is referred to [20] for the graph theoretic notions utilized in this paper. The subsequent analysis are performed under the assumption that the interconnected communication graph is balanced and strongly connected [20], and there exists a unique path [20] between any two distinct agents.

III. Task Space Controlled Synchronization

In this section, the passivity property of the task space trajectory tracking algorithm is first developed [13], [14]. Consequently, this property is then utilized to synchronize manipulators in the task space. The individual systems are required to track a trajectory $X^d(t)$ which is assumed to be twice differentiable. Thus, the signals $\dot{X}^d(t)$, $\ddot{X}^d(t)$ are well defined, and are additionally assumed to be bounded. The dynamic uncertainty in the robot dynamics is represented by the uncertain parameter Θ. It is also assumed that the position of end-effector X is known from either vision systems, position sensors or laser systems, and that the robot is operated in a finite task space where the Jacobian matrix has full rank.

A. Task Space Control Algorithm and Passivity Property

Consider the dynamical system (1), and let the control input [13], [14] be given as

$$u = \hat{M}a + \hat{C}v + \hat{g} - K_t s - J^T K_J^T \tilde{X} + J^T \tau, \tag{5}$$

where $\hat{M}$, $\hat{C}$, and $\hat{g}$ denote the estimates of M, C, and g respectively, $\tilde{X} = X - X^d$ denotes the tracking error, K_t, K_J and Λ are positive definite diagonal matrices, and τ is the synchronizing control that will be subsequently defined. The signals a, v, and s in (5) are defined below (for the non-redundant case where $n = m$),

$$\begin{aligned} v &= J^{-1}(\dot{X}^d - \Lambda(X - X^d)), \\ a &= J^{-1}(\ddot{X}^d - \Lambda(\dot{X} - \dot{X}^d)) + \dot{J}^{-1}(\dot{X}^d - \Lambda(X - X^d)), \\ s &= J^{-1}(-\dot{X}^d + \Lambda(X - X^d)) + \dot{q}, \end{aligned} \tag{6}$$

where $v = \dot{q} - s$ and $a = \dot{v}$.
Defining $r = Js$, the above equation becomes

$$r = (\dot{X} - \dot{X}^d) + \Lambda(X - X^d) = \dot{\tilde{X}} + \Lambda\tilde{X}, \tag{7}$$

where r is the combination of position and velocity tracking errors in the task space.

Using Property 2, the linear parametrization property for Lagrangian systems, the control input can be written as

$$u = Y(q, \dot{q}, v, a)\hat{\Theta} - K_t s - J^T K_J^T \tilde{X} + J^T \tau, \tag{8}$$

where $\hat{\Theta}$ is the estimate of the dynamic parameter vector Θ. Let the estimate be updated as

$$\dot{\hat{\Theta}} = -\Gamma^{-1} Y^T s, \tag{9}$$

where Γ is a positive definite matrix. Substituting (8) into (1), the closed loop system can be written as

$$M\dot{s} + Cs + K_t s = Y\tilde{\Theta} - J^T K_J^T \tilde{X} + J^T \tau, \tag{10}$$

where $\tilde{\Theta} = \hat{\Theta}(t) - \Theta$. The first result in this paper follows.

Lemma 1. *The dynamical system (6), (9), and (10) is passive with (τ, r) as the input-output pair.*

Proof: Consider the positive definite storage function V as

$$V(s, \tilde{X}, \tilde{\Theta}) = \frac{1}{2}\left(s^T M s + \tilde{X}^T K_J \tilde{X} + \tilde{\Theta}^T \Gamma \tilde{\Theta}\right). \tag{11}$$

Differentiating the storage function along the system trajectory and using Property 3, the derivative reduces to

$$\begin{aligned} \dot{V} = {} & s^T J^T \tau - s^T K_t s + \tilde{X}^T K_J \dot{\tilde{X}} - s^T J^T K_J^T \tilde{X} + s^T Y \tilde{\Theta} \\ & + \tilde{\Theta}^T \Gamma \dot{\tilde{\Theta}}. \end{aligned} \tag{12}$$

Using (7), the derivative of $\tilde{X}$ can be written as

$$\dot{\tilde{X}} = -\Lambda\tilde{X} + Js. \tag{13}$$

Substituting the update law (9) and (13) in (12) yields

$$\dot{V} = r^T \tau - s^T K_t s - \tilde{X}^T K_J \Lambda \tilde{X}. \tag{14}$$

Hence, the dynamical system (6), (9), and (10) is passive [21] with (τ, r) as the input-output pair respectively. ∎

B. Task Space Controlled Synchronization

Lemma 1 suggests that the output synchronization results of [8] can be applied to the dynamical system (6), (9), and (10). Considering an N agent multi-agent system, the dynamics of the individual manipulators can be written as

$$\begin{aligned} \dot{\hat{\Theta}}_i &= -\Gamma_i^{-1} Y_i^T s_i, \\ \dot{\tilde{X}}_i &= J_i s_i - \Lambda \tilde{X}_i, \\ \dot{s}_i &= M_i^{-1}(-C_i s_i - K_{ti} s_i + Y_i \tilde{\Theta}_i - J_i^T K_{Ji}^T \tilde{X}_i + J_i^T \tau_i), \end{aligned} \tag{15}$$

where $i = 1, \ldots, N$.

The agents communicate the signals $r_i = J_i^T s_i$ with their neighbors, and are said to output synchronize if

$$\lim_{t\rightarrow\infty}(r_i(t) - r_j(t)) = 0 \quad \forall i, j \in \mathcal{N}_i, \tag{16}$$

where the set $\mathcal{N}_i$ denotes the neighbors of the i^{th} agent. Define $z_i = [\tilde{\Theta}_i \ \tilde{X}_i \ s_i]^T$ as the state of the individual agent and the state of the interconnected multi-agent system is denoted by $Z = [z_1 \ \ldots \ z_N]^T$. Let the synchronizing control be given as

$$\tau_i = \sum_{j\in\mathcal{N}_i} K_s(r_j - r_i) \quad i = 1, \ldots, N, \tag{17}$$

where for the sake of simplicity, the synchronizing gain K_s is assumed to be a positive constant. The main result on task space synchronization is now presented.

Theorem 1. *Consider the dynamical system, described by* (15) *and* (17)*, where the robotic systems are assumed to be non-redundant. If the Jacobian matrix has full rank, and the interconnected communication graph is balanced and strongly connected, then the agents' position and velocities synchronize in the task space, and agents asymptotically follow the desired trajectory.*

Proof: Consider a positive definite storage function for the N agents system as

$$V(Z) = V_1(z_1) + \ldots + V_N(z_N) = \sum_{i=1}^{N} V_i(z_i), \tag{18}$$

where $V_i(z_i)$ is the storage function (11) for the i^{th} agent. Following the proof of Lemma 1, and using (14), the derivative of this storage function can be written as

$$\dot{V}(Z) = \sum_{i=1}^{N} \Big(r_i^T \tau_i - s_i^T K_{ti} s_i - \tilde{X}_i^T K_{Ji} \Lambda \tilde{X}_i \Big) = \sum_{i=1}^{N} \sum_{j \in \mathcal{N}_i} K_s r_i^T (r_j - r_i) - \sum_{i=1}^{N} \Big(s_i^T K_{ti} s_i + \tilde{X}_i^T K_{Ji} \Lambda \tilde{X}_i \Big).$$

As the information exchange graph is balanced [8], the following equation holds.

$$2 \sum_{i=1}^{N} \sum_{j \in \mathcal{N}_i} r_i^T r_i = \sum_{i=1}^{N} \sum_{j \in \mathcal{N}_i} r_i^T r_i + \sum_{i=1}^{N} \sum_{j \in \mathcal{N}_i} r_j^T r_j.$$

Therefore, the derivative of storage function becomes

$$\dot{V} = -\frac{1}{2} \sum_{i=1}^{N} \sum_{j \in \mathcal{N}_i} K_s (r_j - r_i)^T (r_j - r_i) - \sum_{i=1}^{N} \Big(s_i^T K_{ti} s_i + \tilde{X}_i^T K_{Ji} \Lambda \tilde{X}_i \Big) \leq 0.$$

Hence, the zero solution of (15) and (17) is globally stable, and all signals are bounded. Integrating the above equation from $[0, t]$, it is easy to obtain that $\tilde{X}_i$, s_i, and $(r_j - r_i) \in \mathcal{L}_2$, where $j \in \mathcal{N}_i$, $\forall i$. As all signals are bounded, the signals $\dot{\tilde{X}}_i$, $\ddot{\tilde{X}}_i$, and $(\dot{r}_j - \dot{r}_i) \in \mathcal{L}_\infty$. By utilizing Lemma 8.1 in [17], we conclude that $\lim_{t\to\infty} \tilde{X}_i(t) = 0$, $\lim_{t\to\infty} s_i(t) = 0$, $\lim_{t\to\infty} (r_j(t) - r_i(t)) = 0$ $j \in \mathcal{N}_i, \forall i$. Therefore, the agents achieve output synchronization (16), and asymptotically follow the desired trajectory in the task space. Note that

$$r_j - r_i = (\dot{\tilde{X}}_j + \Lambda \tilde{X}_j) - (\dot{\tilde{X}}_i + \Lambda \tilde{X}_i) = (\dot{X}_j - \dot{X}_i) + \Lambda (X_j - X_i) = \dot{e}_{ij} + \Lambda e_{ij}, \tag{19}$$

where $e_{ij} = X_j - X_i$ denotes the synchronization error. The above equation represents an exponentially stable linear system with the input $r_j - r_i$. As shown in [22], it follows that if $r_j - r_i$ is a signal that asymptotically converges to zero, and e_{ij} is bounded then $\lim_{t\to\infty} e_{ij}(t) = 0$ $j \in \mathcal{N}_i$, $\forall i$. Therefore, output synchronization (16) guarantees that the position and the velocities of neighboring agents' end-effectors asymptotically approach each other. As the communication graph is assumed to be strongly connected, all agents synchronize in the task space. ■

C. Task Space Synchronization with Redundant Manipulators

If the robotic manipulators are redundant, that is, $n > m$, the null space of the Jacobian matrix has a minimum dimension of $n - m$. Therefore, the task space motion will not be influenced by the link velocity in the null space. This fact can be utilized in several sub-tasks, such as singularity avoidance, joint limits, and obstacle avoidance, to improve the performance of trajectory tracking [15], [23].

Following [14], [24], the control scheme can be modified as

$$\begin{aligned} v &= J^+(\dot{X}^d - \Lambda(X - X^d)) + (I_n - J^+ J)\psi, \\ a &= J^+(\ddot{X}^d - \Lambda(\dot{X} - \dot{X}^d)) + \dot{J}^+(\dot{X}^d - \Lambda(X - X^d)) \\ &\quad + \frac{d}{dt}[(I - J^+ J)\psi], \\ s &= J^+(-\dot{X}^d + \Lambda(X - X^d)) - (I_n - J^+ J)\psi + \dot{q}, \end{aligned} \tag{20}$$

where $\psi \in R^n$ is a negative gradient of the convex function for the sub-task to be optimized, I_n is $n \times n$ identity matrix, and $J^+ \in R^{n \times m}$ is pseudo-inverse of J, which is defined by $J^+ = J^T (J J^T)^{-1}$, and satisfies $J J^+ = I_m$.

Since pseudo-inverse J^+ has the following properties,

$$J(I_n - J^+ J) = 0 \ , \ (I_n - J^+ J) J^+ = 0 \ , \quad (I_n - J^+ J)(I_n - J^+ J) = I_n - J^+ J,$$

the vector r can be defined analogously (7) to the non-redundant scenario.

According to [15], the sub-task tracking error is defined as $e_N(t) = (I_n - J^+ J)(\dot{q} - \psi)$. Pre-multiplying s in (20) by $(I_n - J^+ J)$ and using the properties above, we can obtain the relation between the sub-task tracking error e_N and s as

$$\begin{aligned} (I_n - J^+ J) s &= (I_n - J^+ J) J^+ (-\dot{X}^d + \Lambda(X - X^d)) \\ &\quad - (I_n - J^+ J)(I_n - J^+ J)\psi + (I_n - J^+ J)\dot{q} \\ &= (I_n - J^+ J)(\dot{q} - \psi) = e_N. \end{aligned} \tag{21}$$

Thus, if $\lim_{t\to\infty} s(t) = 0$, then the sub-task tracking error also approaches the origin.

As the matrix $(I_n - J^+ J)$ satisfies the property that $J(I_n - J^+ J) = 0$, for redundant robots, the modified signals a, v, and s in (20) are employed for the control input (5) in the control task. Hence, following the proof of Theorem 1, the convergence of task space synchronization errors, and the sub-task tracking errors to the origin is guaranteed by the control scheme. The next result formalizes the above discussion.

Corollary 1. *Consider the dynamical system described by (15) and (17), where one or more manipulators may have redundant degrees-of-freedom. If the interconnected communication graph is balanced and strongly connected, then the manipulators synchronize in the task space, and asymptotically follow the desired trajectory. Additionally, the sub-task tracking errors for the redundant manipulators converge to the origin.*

IV. Task Space Synchronization with Time Delays

When communicating over unreliable communication networks, such as a wireless network, it is possible to have time-varying communication delays between the robotic systems. In the subsequent analysis, it is assumed that $T_{ji}(t)$ denotes the time-varying time delays from the j^{th} agent to the i^{th} agent. The time delays are assumed to be continuously differentiable, bounded ($0 < T_{ij}(t) \leq T_{M_{ij}} < \infty$), and satisfy

$$\dot{T}_{ij}(t) \leq \bar{T}_{ij} < 1 \quad j \in \mathcal{N}_i, \ i = 1, \cdots, N, \tag{22}$$

where $\bar{T}_{ij}$ is a nonnegative constant. The condition (22) implies that the time-varying delays cannot grow faster than time itself, but there is no constraint on the decreasing rate of delays, as long as the delays are continuously differentiable and bounded.

Definition In the presence of delays, the manipulators are said to delay-output synchronize if

$$\lim_{t\to\infty} (r_j(t - T_{ji}(t)) - r_i(t)) = 0 \quad \forall i, j \in \mathcal{N}_i, \tag{23}$$

where $r_j(t - T_{ji}(t))$ is the delayed output of the j^{th} agent received by the i^{th} agent .

To achieve delay-output synchronization, define positive constant gains dependent on the maximum rate of change of delays [25] as

$$d_{ji}^2 \leq (1 - \bar{T}_{ji}) \quad j \in \mathcal{N}_i, \ i = 1, \cdots, N. \tag{24}$$

Let the delay-synchronizing control be given by

$$\tau_i = \sum_{j \in \mathcal{N}_i} K_s \Big(d_{ji}^2 r_j(t - T_{ji}(t)) - \big(\frac{d_{ji}^2}{2} + \frac{1}{2}\big) r_i \Big). \tag{25}$$

In the proposed control algorithm, $r_j(t-T_{ji}(t))$ indicates the output signal that was transmitted $T_{ji}(t)$ units of time earlier by the j^{th} agent, and is received at the current time instance t by the i^{th} agent. Hence, the control input defined above utilizes the delayed output, and does not require exact knowledge of time-varying delays. The result on task space synchronization with communication time-varying delays follows.

Theorem 2. *Consider the dynamical system, described by (15) and (25), where only non-redundant manipulators are considered. If the Jacobian matrix has full rank, and the interconnected communication graph is balanced and strongly connected, then the manipulators delay output synchronize and asymptotically follow the desired trajectory. Furthermore, in the presence of time-varying delays, the synchronization errors in task space are bounded, and asymptotically converge to zero.*

Proof: Consider a positive definite storage functional for the delayed system as

$$V(Z) = \sum_{i=1}^{N} V_i(z_i) + \frac{K_s}{2}\sum_{i=1}^{N}\sum_{j\in\mathcal{N}_i}\int_{t-T_{ji}(t)}^{t} r_j^T(\sigma) r_j(\sigma) d\sigma,$$

where the storage function $V_i(z_i)$ is given by (11) for i^{th} agent. Taking the time derivative along the trajectories of the system yields

$$\dot{V} = \sum_{i=1}^{N}\Big(r_i^T\tau_i - s_i^T K_{ti} s_i - \tilde{X}_i^T K_{Ji}\Lambda\tilde{X}_i\Big) + \frac{K_s}{2}\sum_{i=1}^{N}\sum_{j\in\mathcal{N}_i}\Big(r_j^T r_j - (1-\dot{T}_{ji}(t)) r_j^T(t-T_{ji}(t)) r_j(t-T_{ji}(t))\Big).$$

Substituting the delay-synchronizing control (25) into the inequality above, the derivative becomes

$$\dot{V} \le \frac{K_s}{2}\sum_{i=1}^{N}\sum_{j\in\mathcal{N}_i}\Big(2d_{ji}^2 r_i^T r_j(t-T_{ji}(t)) - d_{ji}^2 r_i^T r_i - r_i^T r_i + r_j^T r_j - d_{ji}^2 r_j(t-T_{ji}(t))^T r_j(t-T_{ji}(t))\Big) - \sum_{i=1}^{N}(s_i^T K_{ti} s_i + \tilde{X}_i^T K_{Ji}\Lambda\tilde{X}_i).$$

As the graph is balanced $\sum_{i=1}^{N}\sum_{j\in\mathcal{N}_i} r_i^T r_i = \sum_{i=1}^{N}\sum_{j\in\mathcal{N}_i} r_j^T r_j$, the derivative of the storage function becomes

$$\dot{V} \le -\sum_{i=1}^{N}(s_i^T K_{ti} s_i + \tilde{X}_i^T K_{Ji}\Lambda\tilde{X}_i) - \frac{K_s}{2}\sum_{i=1}^{N}\sum_{j\in\mathcal{N}_i} d_{ji}^2\big(r_i - r_j(t-T_{ji}(t))\big)^T\big(r_i - r_j(t-T_{ji}(t))\big).$$

Hence, all signals in the dynamical system (15) and (25) are bounded. Following the arguments as in Theorem 1, it can be obtained that the signals $\tilde{X}_i$, s_i, $r_j(t-T_{ji}(t))-r_i \in \mathcal{L}_2, \dot{\tilde{X}}_i, \ddot{\tilde{X}}_i, \dot{r}_j(t-T_{ji}(t))-\dot{r}_i \in \mathcal{L}_\infty$, and it can be shown that $\lim_{t\to\infty}\tilde{X}_i(t)=0$, $\lim_{t\to\infty} s_i(t)=0$ and $\lim_{t\to\infty}(r_j(t-T_{ji}(t)) - r_i(t)) = 0 \quad \forall i,j \in \mathcal{N}_i$. Therefore, the synchronizing control and communication assumption guarantee delay-output synchronization (23) in the presence of time-varying delays in the communication.

By defining $e_{ji}^d := X_j(t-T_{ji}(t)) - X_i(t) + X^d(t) - X^d(t-T_{ji}(t))$, the delay-output synchronization can be further rewritten as

$$\begin{aligned} r_j(t-T_{ji}(t)) - r_i &= \Big(\big(\dot{X}_j(t-T_{ji}(t)) - \dot{X}^d(t-T_{ji}(t))\big) \\ &\quad +\Lambda\big(X_j(t-T_{ji}(t)) - X^d(t-T_{ji}(t))\big)\Big) \\ &\quad -\Big((\dot{X}_i - \dot{X}^d) + \Lambda(X_i - X^d)\Big) \\ &= \Big(\dot{X}_j(t-T_{ji}(t)) - \dot{X}_i + \dot{X}^d - \dot{X}^d(t-T_{ji}(t))\Big) \\ &\quad +\Lambda\Big(X_j(t-T_{ji}(t)) - X_i + X^d - X^d(t-T_{ji}(t))\Big) \\ &= \dot{e}_{ji}^d + \Lambda e_{ji}^d. \end{aligned} \tag{26}$$

Following the statement in [5], as $r_j(t-T_{ji}(t)) - r_i(t)$ converges asymptotically to zero and e_{ji}^d is bounded, $\lim_{t\to\infty} e_{ji}^d(t) = 0,\ j \in \mathcal{N}_i, \forall i$. Since e_{ji}^d and $\tilde{X}_j$ are bounded, and

$$\begin{aligned} e_{ji}^d &= X_j(t-T_{ji}(t)) - X_i + X^d - X^d(t-T_{ji}(t)) \\ &= (X_j - X_i) + \tilde{X}_j(t-T_{ji}(t)) - \tilde{X}_j, \end{aligned} \tag{27}$$

the synchronization errors in task space, $X_j - X_i,\ j \in \mathcal{N}_i, \forall i$, are bounded. Using (27) and letting $t \to \infty$, we obtain that $\lim_{t\to\infty}(X_j(t) - X_i(t)) = 0$. ■

Theorem 2 demonstrates that by utilizing the delay-synchronizing control (25), it is possible to synchronize heterogeneous robotic manipulators under time-varying communication delays. Based on the assumption that time delays in the communication channels are continuous, the derivative of the time-varying delays is less than one due to the causality implications [26]. Therefore, the delays may be large, but are required to have slow variations as dictated by the assumption (22). In practical implementation, it is possible that there may be packet losses, sharply varying delays, and packet ordering in the system. The incoming data can be buffered, and appropriate communication management modules can be utilized [27] to address this problem. As the application of these methods is beyond the scope of this paper, the readers are referred to [27]–[29] for more details.

The delay-synchronizing control (25) in Theorem 2 is applicable for guaranteeing output synchronization by choosing $d_{ij} = 1$ if the time delays in the communication channels are constant. In addition, if there are redundant manipulators in the interconnected system, the next corollary follows from the analysis in Section III-C.

Corollary 2. *Consider the dynamical system described by (15) and (25), where one or more redundant manipulators may cooperate with other robots. If the interconnected communication graph is balanced and strongly connected, then the agents delay output synchronize, and asymptotically follow the desired trajectory. Additionally, the convergence of sub-task tracking errors of redundant manipulators is guaranteed.*

V. Validation Results

A. Simulations: Synchronization with Redundant Manipulators

In this subsection, simulations are utilized to analyze the efficacy of the previously described synchronization algorithms. The multi-agent system consists of two 2-link, and two 3-link planar manipulators. Since all the robotic agents in the system are planar manipulators, the control goal is to synchronize the end-effectors in the X-Y plane while ensuring that they follow the desired trajectory. The agents are interconnected using a ring topology as shown in Figure 1 (a), where agents 2 and 3 are the 2-link manipulators, and agents 1 and 4 are the 3-link redundant manipulators.

The dynamics of the planar manipulators are adapted from [17]. In the simulations, the parameters are listed in Table I with $g = 9.8$, where m_{ij} denotes the mass of the j^{th} link for the i^{th} agent, l_{ij} denotes the length of the j^{th} link for the i^{th}, and I_{ij} denotes the moment of inertia of the j^{th} link for the i^{th} agent. The initial joint angles are assigned as $q_1(0) = [0.8, 1.2, 0.4]$ rad, $q_2(0) = [0.5, 0.8]$ rad, $q_3(0) = [-0.8, 1.8]$ rad, and $q_4(0) = [1.7, 1.6, 0.9]$ rad. The desired trajectory for the end-effectors is given as $X(t) = 1.2 + 0.5\sin(t)$ cm, and $Y(t) = 1 + 0.3\cos(t)$ cm. Furthermore, in the simulations, the sub-task function for redundant manipulator agent 1 is selected as $\psi_1 = -20(q_{11} - 1)$, which is the negative gradient of

TABLE I: Parameters utilized in simulations.

Agent	Length of link	Mass	Inertia
1^{st}	$l_{11} = 1.2$, $l_{12} = 0.9$, $l_{13} = 0.8$	$m_{11} = 1.1$, $m_{12} = 0.8$, $m_{13} = 0.5$	$I_{11} = 0.012$, $I_{12} = 0.135$, $I_{13} = 0.025$
2^{nd}	$l_{21} = 1.5$, $l_{22} = 1.4$	$m_{21} = 1.2$, $m_{22} = 0.6$	$I_{21} = 0.24$, $I_{22} = 0.12$
3^{rd}	$l_{31} = 1.5$, $l_{32} = 0.6$	$m_{31} = 0.8$, $m_{32} = 0.75$	$I_{31} = 0.035$, $I_{32} = 0.08$
4^{th}	$l_{41} = 0.9$, $l_{42} = 0.8$, $l_{43} = 0.7$	$m_{41} = 1.1$, $m_{42} = 0.9$, $m_{43} = 0.8$	$I_{41} = 0.12$, $I_{42} = 0.023$, $I_{43} = 0.31$

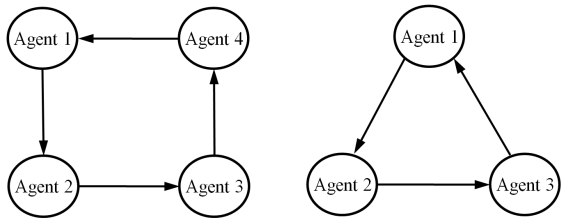

(a) Topology for simulations (b) Topology for experiments

Fig. 1: Balanced communication topologies for the simulations and experiments. The agents for the experimental results are PHANToM Omni haptic devices.

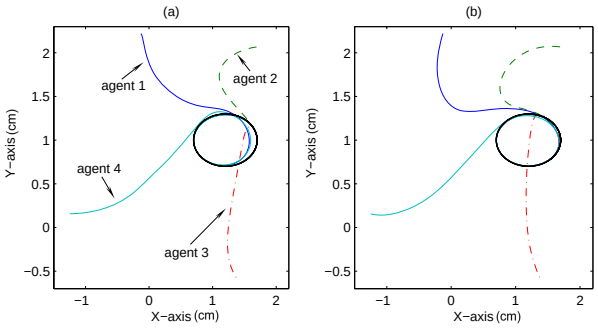

Fig. 2: Trajectory of the end-effectors. (a) $K_s = 0$, without synchronization. (b) $K_s = 10$, with synchronizing control (17).

$(10(q_{11} - 1))^2$, where q_{11} is the first joint angle of agent 1. This sub-task tracking function forces the first joint of agent 1 towards $q_{11} = 1$ rad. In the case of agent 4, $\psi_4 = \frac{\partial}{\partial q}(\det(J_4 J_4^T))$ is selected as in [15] for increasing the manipulability of the manipulator.

The control gains for the subsequent simulations are given as $K_{t1} = K_{t4} = \text{diag}\{5, 5, 5\}$, $K_{t2} = K_{t3} = \text{diag}\{5, 5\}$, $\Lambda = \text{diag}\{10, 10\}$, and $K_{Ji} = \text{diag}\{2, 2\}$, $i = 1, 2, 3, 4$. In the absence of synchronization, $K_s = 0$, manipulators follow the desired trajectory in the task space as shown in Figure 2 (a). If the synchronizing gain $K_s = 10$, agents synchronize and then follow the trajectory as shown in Figure 2 (b). For the redundant manipulators, agents 1 and 4, the null space can be utilized in several sub-tasks. Based on the sub-task functions described above, the first joint of agent 1 moves towards a steady state configuration of 1 rad as shown in Figure 3, and the sub-task for agent 4 increases the manipulability as shown in Figure 4.

We next discuss the simulation results for task space synchronization in the presence of communication delays. The agents communicate the signal r_i to their neighbors with communication delays $T_{12}(t) = T_{23}(t) = 0.6 + 0.5\sin(t/2)$ sec, and $T_{34}(t) = T_{41}(t) = 0.3 + 0.2\sin(t/2)$ sec, which satisfy the assumption that $\dot{T}_i(t) \leq 1, i = 1, 2, 3, 4$. The gains for the time-varying delays, d_{ji}, $\forall i, j$, are assumed to be equal for the sake of simplicity, and are selected as $d_{ji} = 0.5 \quad j \in \mathcal{N}_i$, $i = 1, 2, 3, 4$. If the synchronizing controller in (17) is utilized without any additional compensation, as shown in Figure 5 (a), there are abnormal oscillations resulting from

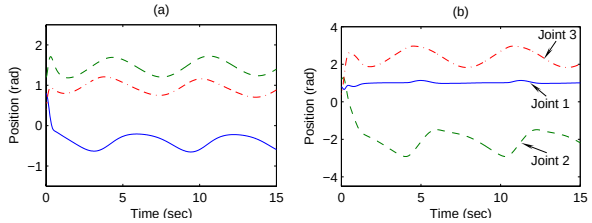

Fig. 3: Joint angles of the agent 1, which is a redundant manipulator. (a) Without sub-task control. (b) With sub-task control, the first joint of agent 1 was forced toward 1rad.

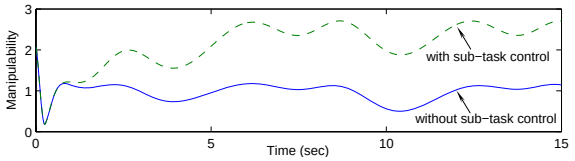

Fig. 4: Manipulability of agent 4. Sub-task control increases the manipulability in the task space.

the influence of time-varying communication delays. However, if the controller was replaced by (25), the manipulators synchronize without perturbations, and follow the desired trajectory as shown in Figure 5 (b). The synchronization errors between the agents are shown in Figure 6 and 7. Using the time-varying synchronizing controller (25), agents achieve synchronization faster with better performance as compared to the controller described in (17).

B. Experiments: Synchronization with Non-Redundant Manipulators

The proposed control algorithms are also implemented using non-redundant PHANToM Omni haptic devices. The Omni is a cost-effective device that can be utilized to test, and verify control schemes. For the subsequent experiments, the detachable stylus of the Omni was removed, and the last two joints were constrained to reduce the influence of the unactuated links on the robot dynamics.

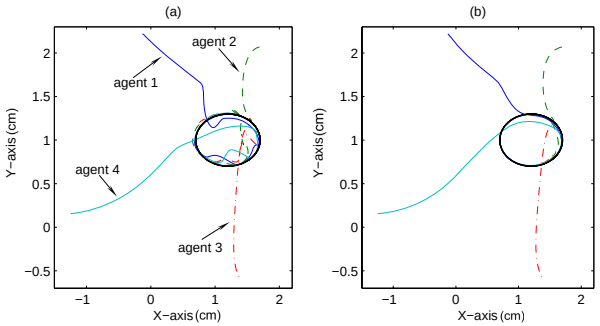

Fig. 5: Trajectory of the end-effectors with time-varying communication delay. (a) Use of non-delay-synchronizing controller (17). (b) Use of delay-synchronizing controller (25).

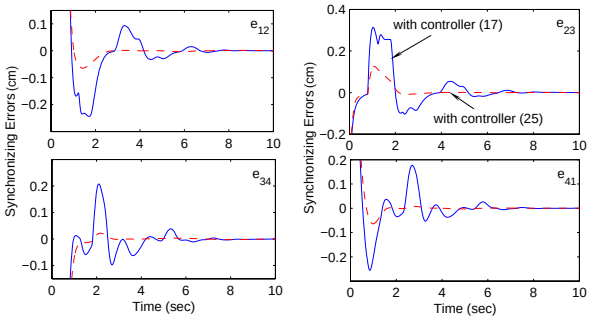

Fig. 6: X-axis synchronization errors in the presence of time-varying communication delay.

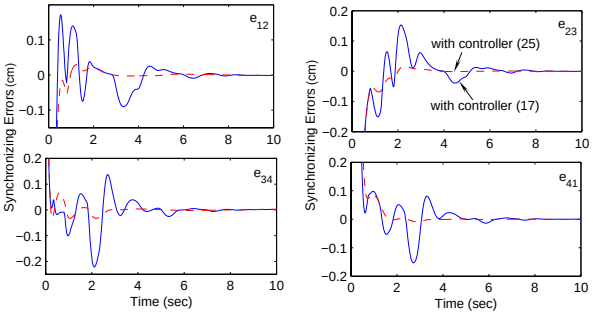

Fig. 7: Y-axis synchronization errors in the presence of time-varying communication delay.

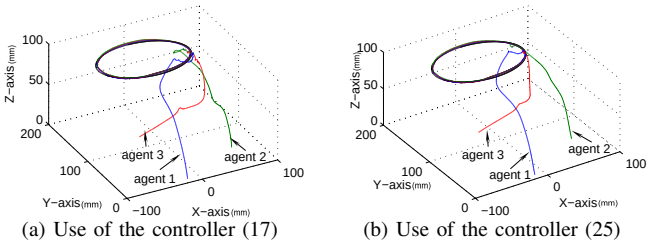

(a) Use of the controller (17) (b) Use of the controller (25)

Fig. 8: Experimental results for task space synchronization with time-varying delays.

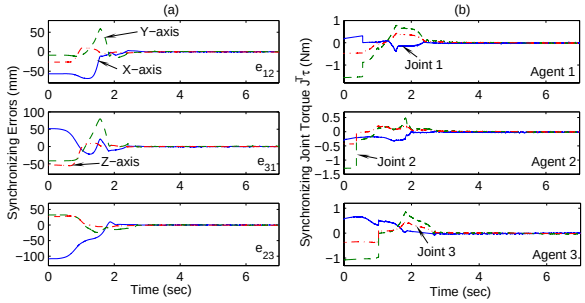

Fig. 9: When the delay-synchronizing controller (25) is used, the above plots illustrate (a) The synchronization errors (b) The synchronizing torque $J^T\tau$.

Hence, the Omni performs as a fully actuated manipulator with three revolute joints.

In the experiments, three fully actuated manipulators interconnected with a balanced topology (see Figure 1 (b)), are controlled by a desktop computer. The control program was written in C with the use of OpenHaptics API, a software by SensAble Technologies [30]. It was assumed that all signals acquired from the API are reliable. The data collection and control input rate ran at a sampling rate of 1kHz, and the position and velocity of the end-effector was obtained from OpenHaptics API. The desired trajectory for the end-effector was chosen as $X(t) = 60\sin(0.2\pi t)$ mm, $Y(t) = 150 + 40\cos(0.2\pi t)$ mm, and $Z(t) = 80$ mm due to the workspace limitations. Moreover, time-varying delays were artificially added to the communication path and were given as $T_{12}(t) = 0.3 + 0.2\sin(t)$ sec, $T_{23}(t) = 0.6 + 0.5\sin(t)$ sec, and $T_{31}(t) = 0.4 + 0.3\sin(t)$ sec. The gains d_{ij} utilized to compensate for the time-varying delays were chosen to be equal with $d_{ji} = 0.7 \quad j \in \mathcal{N}_i,\ i = 1, 2, 3$.

The experiments were conducted using the control scheme (8), where the regressor matrix Y and parameter vector Θ are listed in the Appendix. The control parameters are given as Λ =diag{10, 10, 10}, K_{ti} =diag{0.1, 0.15, 0.15}, K_{Ji} =diag{0.1, 0.15, 0.14}, Γ_i^{-1} =diag{0.01, 0.01, 0.001, 0.001, 0.01, 0.005, 1.5, 2} $i = 1, 2, 3$, and synchronizing gain $K_s = 0.006$. The dynamic parameters are updated using the adaptive control in (9) with $\hat{\Theta}_1(0) = [0.1, 0, 0.2, 0.4, 0.4, 0.1, 70, 80]$, $\hat{\Theta}_2(0) = [0.1, 0, 0.2, 0.4, 0.4, 0.1, 80, 60]$, and $\hat{\Theta}_3(0) = [0.1, 0, 0.2, 0.4, 0.4, 0.1, 75, 70]$.

If the synchronizing controller in (17) was used, time-varying delays resulted in abnormal oscillations as shown in Figure 8 (a). However, if the controller was replaced by (25), the manipulators synchronized faster with better performance, as shown in Figure 8 (b). For the synchronizing controller (25), the synchronizing errors between agents are shown in Figure 9 (a), and Figure 9 (b) illustrates the synchronizing joint torque $J^T\tau$. As seen from these results, three manipulators can achieve task space synchronization in the presence of time-varying delays with bounded synchronizing torques. Additionally, the synchronizing errors in the task space are bounded, and asymptotically converge to zero. Furthermore, the estimates of the dynamic parameters are shown in Figure 10, where Θ_i denotes the i^{th} entry of Θ. These experimental results demonstrate that the interconnected manipulators can achieve task space synchronization in the presence of dynamic uncertainties, and time-varying communication delays by utilizing the control algorithms developed in this paper.

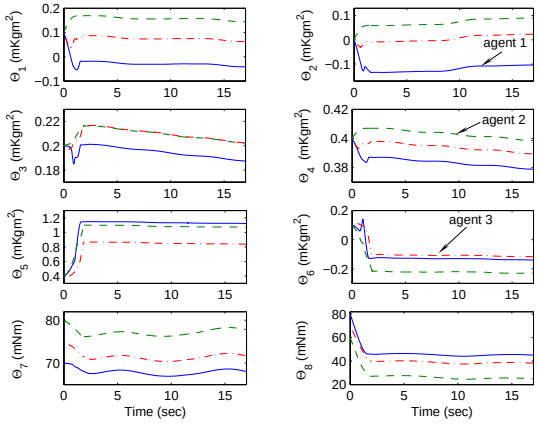

Fig. 10: The control algorithm results in bounded estimates despite the time-varying delays in the closed loop system.

$$Y = \begin{bmatrix} a_1c_{22} - s_{22}(v_2\dot{\theta}_1 - v_1\dot{\theta}_2) & v_1 s_{22}\dot{\theta}_1 & 0 \\ -s_{22,23}\dot{\theta}_1(v_2+v_3) - v_1 s_{22,23}(\dot{\theta}_2 - \dot{\theta}_3) & v_1 s_{22,23}\dot{\theta}_1 & v_1 s_{22,23}\dot{\theta}_1 \\ +a_1 c_{22,23} & & \\ a_1(s_{22,3}+s_3) + \frac{1}{2}c_3(v_1\dot{\theta}_3 + v_3\dot{\theta}_1) & s_3(2a_2+a_3) - v_1 c_{22,3}\dot{\theta}_1 & a_2 s_3 - (\frac{1}{2}v_1 c_{22,3} + \frac{1}{2}v_1 c_3)\dot{\theta}_1 \\ +c_{22,3}(v_2\dot{\theta}_1 + \frac{1}{2}v_3\dot{\theta}_1 + v_1\dot{\theta}_2 + \frac{1}{2}v_1\dot{\theta}_3) & +c_3(v_3\dot{\theta}_2 + v_3\dot{\theta}_3 + v_2\dot{\theta}_3) & -c_3 v_2\dot{\theta}_2 \\ a_1 & 0 & 0 \\ 0 & a_2 & 0 \\ 0 & a_3 & a_2 + a_3 \\ 0 & s_{2,3} & s_{2,3} \\ 0 & c_2 & 0 \end{bmatrix}^T \tag{28}$$

VI. Conclusions

In this paper, task space controlled synchronization for heterogeneous robotic manipulators with time-varying communication delays and dynamic uncertainties was studied. It was demonstrated that robotic manipulators, communicating with each other over balanced graphs, can achieve task space synchronization when following a nominal trajectory. The synchronization results were developed for both redundant and non-redundant manipulators. If one or more of the robotic systems were redundant, the additional degrees-of-freedom were exploited to achieve several sub-tasks, such as singularity and obstacle avoidance. The robustness of the synchronization algorithm to time-varying delays in communication was also investigated. The efficacy of the proposed control algorithms was studied by numerical simulations, and experiments on PHANToM Omni robotic systems. Future work will consider the effect of different communication topologies on the performance of the system, and study task space synchronization with time-varying delays when a human operator is present in the closed loop system [31], [32].

Appendix

$$\Theta = \begin{bmatrix} \frac{1}{2}m_3 l_1^2 + \frac{1}{8}m_2 l_1^2 + \frac{1}{2}I_{2z} - \frac{1}{2}I_{2y} \\ -\frac{1}{8}m_3 l_2^2 - \frac{1}{2}I_{3y} + \frac{1}{2}I_{3z} \\ \frac{1}{2}m_3 l_1 l_2 \\ \frac{1}{8}m_2 l_1^2 + \frac{1}{8}m_3 l_2^2 + \frac{1}{2}m_3 l_1^2 + \frac{1}{2}I_{2z} + \frac{1}{2}I_{3y} + \frac{1}{2}I_{2y} \\ +\frac{1}{2}I_{3z} + I_{1z} \\ \frac{1}{4}m_3 l_2^2 + m_3 l_1^2 + \frac{1}{4}m_2 l_1^2 + I_{2x} + I_{3x} \\ \frac{1}{4}m_3 l_2^2 + I_{3x} \\ \frac{1}{2}m_3 g l_2 \\ \frac{1}{2}m_3 g l_1 + \frac{1}{2}m_2 g l_1 \end{bmatrix} \tag{29}$$

The vector of unknown parameters $\Theta \in R^{\,8}$, and the regressor matrix $Y(\theta, \dot{\theta}, v, a) \in R^{\,3\times 8}$ of the PHANToM Omni for the implementation of proposed control scheme are given in this section. The matrix Y, and the vector Θ and are shown in (28) and (29), respectively, where $a = [a_1,\ a_2,\ a_3]$ and $v = [v_1,\ v_2,\ v_3]$ are defined in (6), l_i denotes the length of link i, m_i denotes the mass of link i, I_{ij} denotes the moment of inertia of link i in j axis for $i = 1,\ 2,\ 3$ and $j = x,\ y,\ z$. Denoting $\theta_i(t)$ as the joint angles of Omni for $i = 1, 2, 3$, c_2, s_3, c_3, s_{22}, c_{22}, $s_{2,3}$, $s_{22,3}$, $s_{22,23}$, and $c_{22,23}$ are shorthand for $cos(\theta_2)$, $sin(\theta_3)$, $cos(\theta_3)$, $sin(2\theta_2)$, $cos(2\theta_2)$, $sin(\theta_2+\theta_3)$, $sin(2\theta_2+\theta_3)$, $sin(2\theta_2+2\theta_3)$, and $cos(2\theta_2+2\theta_2)$, respectively.

Acknowledgment

The authors would like to thank the Editors and the anonymous reviewers for their valuable comments and suggestions that led to significant improvements in the presentation of this paper.

References

[1] H. Nijmeijer and A. Rodriguez-Angeles, *Synchronization of mechanical systems*. River Edge, NJ: World Scientific, 2003.

[2] A. Rodriguez-Angeles and H. Nijmeijer, "Mutual synchronization of robots via estimated state feedback: a cooperative approach," *IEEE Transactions on Control Systems Technology*, vol. 12, no. 4, pp. 542–554, Jul. 2004.

[3] S.-J. Chung and J.-J. E. Slotine, "Cooperative robot control and concurrent synchronization of Lagrangian systems," *IEEE Transactions on Robotics*, vol. 25, no. 3, pp. 686–700, Jun. 2009.

[4] S.-J. Chung, U. Ahsun, and J.-J. E. Slotine, "Application of synchronization to formation flying spacecraft: Lagrangian approach," *AIAA Journal of Guidance, Control and Dynamics*, vol. 32, no. 2, pp. 512–526, Mar.-Apr. 2009.

[5] N. Chopra and Y.-C. Liu, "Controlled synchronization of mechanical systems," in *Proceedings of ASME Dynamic Systems and Control Conference*, Oct. 2008, pp. 1221–1228.

[6] A. Pogromsky and H. Nijmeijer, "Cooperative oscillatory behavior of mutually coupled dynamical systems," *IEEE Transactions on Circuits and Systems I*, vol. 48, no. 2, pp. 152–162, Feb. 2001.

[7] G.-B. Stan and R. Sepulchre, "Analysis of interconnected oscillators by dissipativity theory," *IEEE Transactions on Automatic Control*, vol. 52, no. 2, pp. 256–270, Feb. 2007.

[8] N. Chopra and M. W. Spong, "Passivity-based control of multi-agent systems," in *Advances in Robot Control: From Everyday Physics to Human-Like Movements*, S. Kawamura and M. Svinin, Eds. New York: Springer Verlag, 2006, pp. 107–134.

[9] ——, "Output synchronization of nonlinear systems with time delay in communication," in *Proceedings of IEEE Conference on Decision and Control*, Dec. 2006, pp. 4986–4992.

[10] N. Chopra, M. W. Spong, and R. Lozano, "Synchronization of bilateral teleoperators with time delay," *Automatica*, vol. 44, no. 8, pp. 2142–2148, Aug. 2008.

[11] H. Kawada, K. Yoshida, and T. Namerikawa, "Synchronized control for teleoperation with different configurations and communication delay," in *Proceedings of IEEE Conference on Decision and Control*, Dec. 2007, pp. 2546–2551.

[12] N. Nath, E. Tatlicioglu, and D. M. Dawson, "Teleoperation with kinematically redundant robot manipulators with sub-task objectives," *Robotica*, vol. 27, pp. 1027–1038, 2009.

[13] J.-J. Slotine and W. P. Li, "Adaptive manipulator control: A case study," *IEEE Transactions on Automatic Control*, vol. 33, no. 11, pp. 995–1003, Nov. 1988.

[14] E. Zergeroglu, D. M. Dawson, I. Walker, and P. Setlur, "Nonlinear tracking control of kinematically redundant robot manipulators," *IEEE/ASME Transactions on Mechatronics*, vol. 9, no. 1, pp. 129–132, Mar. 2004.

[15] P. Hsu, J. Hauser, and S. Sastry, "Dynamic control of redundant manipulators," *Journal of Robotic Systems*, vol. 6, pp. 133–148, Apr. 1989.

[16] J. P. Richard, "Time-delay systems: an overview of some recent advances and open problems," *Automatica*, vol. 39, no. 10, pp. 1667–1694, Oct. 2003.

[17] M. W. Spong, S. Hutchinson, and M. Vidyasagar, *Robot Modeling and Control*. New York: John Wiley & Sons, Inc., 2006.

[18] W. E. Dixon, "Adaptive regulation of amplitude limited robot manipulators with uncertain kinematics and dynamics," *IEEE Transactions on Automatic Control*, vol. 52, no. 3, pp. 488–493, Mar. 2007.

[19] C. C. Cheah, C. Liu, and J.-J. E. Slotine, "Adaptive tracking control for

robots with unknown kinematic and dynamic properties," *International Journal of Robotics Research*, vol. 25, no. 3, pp. 283–296, Mar. 2006.
[20] C. Godsil and G. Royle, *Algebraic Graph Theory*. New York: Springer, 2001.
[21] H. K. Khalil, *Nonlinear Systems*. New Jersey: Prentice Hall, 2002.
[22] E. D. Sontag, "A remark on the converging-input converging-state property," *IEEE Transactions on Automatic Control*, vol. 48, no. 2, pp. 313–314, Feb. 2003.
[23] E. Tatlicioglu, M. L. McIntyre, D. M. Dawson, and I. D. Walker, "Adaptive non-linear tracking control of kinematically redundant robot manipulators," *International Journal of Robotics and Automation*, vol. 23, no. 2, pp. 98–105, Mar. 2008.
[24] T. Yoshikawa, "Analysis and control of robot manipulators with redundancy," in *Robotics Research: The First International Symposium on Robotics Research*, M. Brady and R. Paul, Eds. Cambridge, MA: MIT Press, 1984, pp. 735–747.
[25] R. Lozano, N. Chopra, and M. W. Spong, "Passivation of force reflecting bilateral teleoperation with time varying delay," *Mechatronics '02*, 2002.
[26] M. Krstic, *Delay Compensation for Nonlinear, Adaptive, and PDE Systems*. Birkhauser, 2009.
[27] N. Chopra, P. Berestesky, and M. W. Spong, "Bilateral teleoperation over unreliable communication networks," *IEEE Transactions on Control Systems Technology*, vol. 16, no. 2, pp. 304–313, Mar. 2008.
[28] K. Kosuge, H. Murayama, and K. Takeo, "Bilateral feedback control of telemanipulators via computer network," in *Proceedings of IEEE Conference on Intelligent Robots and Systems*, 1996, pp. 1380 –1385.
[29] B. Sinopoli, C. Sharp, L. Schenato, S. Schaffert, and S. Sastry, "Distributed control applications within sensor networks," *Proceedings of the IEEE*, vol. 91, no. 8, pp. 1235–1246, Aug. 2003.
[30] *http://www.sensable.com*, SensAble Technologies.
[31] O. M. Palafox and M. W. Spong, "Bilateral teleoperation of a formation of nonholonomic mobile robots under constant time delay," in *Proceedings of IEEE/RSJ International Conference on Intelligent Robots and Systems*, Oct. 2009, pp. 2821–2826.
[32] E. Nuno and L. Basanez, "Nonlinear bilateral teleoperation: Stability analysis," in *Proceedings of IEEE International Conference on Robotics and Automation*, Jul. 2009, pp. 3718–3723.